Electronic Supplementary Information

An Ultrasensitive Flow Cytometric Immunoassay Based on Bead Surface-Initiated Template-Free DNA Extension

Liping Zhu, Desheng Chen, Xiaohui Lu, Yan Qi, Pan He, Chenghui Liu, Zhengping Li*

Key Laboratory of Analytical Chemistry for Life Science of Shaanxi Province; Key Laboratory of Applied Surface and Colloid Chemistry, Ministry of Education; School of Chemistry and Chemical Engineering, Shaanxi Normal University, Xi'an 710119, Shaanxi Province, P. R. China

Corresponding author: Prof. Dr. Chenghui Liu

Email: liuch@snnu.edu.cn (C. Liu)

Phone/Fax: +86 29 81530859

List of Contents

1. Synthesis and characterization of the 16 nm AuNPs

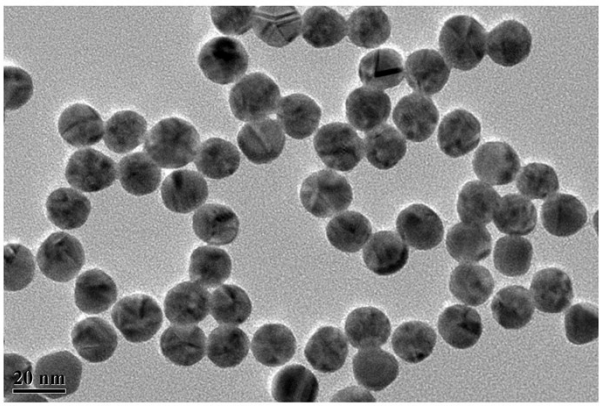

Fig. S1. The representative TEM image of the prepared AuNPs.

The gold nanoparticles (AuNPs) were prepared following the well-established protocol.[S1] Briefly, all glassware was firstly cleaned in the freshly prepared $K_2Cr_2O_7$-H_2SO_4 (3:1) solution, thoroughly rinsed with ultrapure water, and then dried prior to use. 100 mL of $HAuCl_4$ solution (0.01%) was boiled under vigorous stirring. Then, 2 mL of 1% trisodium citrate solution was pipetted into the boiling solution quickly, and kept boiling for 15 min under stirring. Along with the formation of AuNPs, the solution color changed from pale yellow to brilliant red. After cooled down to room temperature, the colloidal AuNPs was stored at 4 °C. The as-prepared AuNPs were characterized on a JEM-2100 high resolution transmission electron microscopy (HR-TEM, JEOL). The HR-TEM image of AuNPs (Fig. S1) reveals a highly monodispersed AuNPs with an average diameter of ~16 nm.

2. Optimization of the amount of TdT

To achieve the best analytical performance of the proposed method, the effect of TdT dosage was investigated by varying the TdT from 0.2 U to 10 U. As shown in Fig. S2a, the PSA-aroused fluorescence intensity of the MBs increases sharply when TdT increases from 0.2 U to 10 U. Meanwhile, the fluorescence responses of the blank control (without PSA) also show an increasing tendency along with the increase of TdT dosage. In this study, the highest S/B ratio produced by PSA to that of the blank control is obtained at 1.0 U of TdT (Fig. S2b). Taking into consideration of relatively low background and high PSA-produced signal to realize better discrimination of the target

from the blank, 1.0 U of TdT is selected for PSA analysis in this work.

It should be noted that if 1.0 U TdT is used for PSA analysis, the blank control shows a relatively high signal under the FL1 voltage of 465 V for FCM measurement (as shown in image (III) of Fig. S2a). So, when evaluating the analytical performance of the proposed TdT-FCI under the optimized experimental conditions (Fig. 4 in the main text), the FL1 Voltage for the FCM analysis was rationally lowered down to 420 V to ensure a low blank signal and a wider dynamic range for PSA analysis.

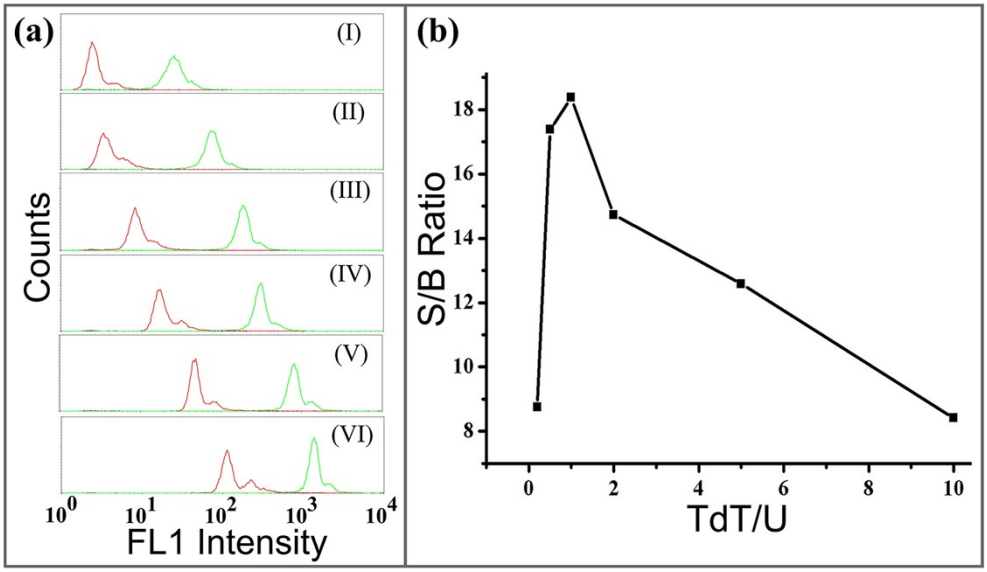

Fig. S2. Optimization of TdT dosage for the detection of PSA. (a) Fluorescence histograms of the MBs incubated with 1 ng/mL PSA (green) in comparison with those of blank control (without PSA, red) in the presence of varying dosage of TdT. (I) 0.2 U; (II) 0.5 U; (III) 1 U; (IV) 2 U; (V) 5 U; (VI) 10 U. (b) The corresponding S/B ratio under different TdT concentrations. S/B ratio refers to the ratio of 1 ng/mL PSA-aroused MFI value to that of blank control. The other experimental conditions: dTTP, 1 mM; FL1 Voltage in the FCM measurement, 465 V.

3. Optimization of the ratio of mAb2 and ODN on the AuNPs

In the proposed TdT-FCI strategy, the ratio of mAb2 to ODN on the AuNPs is a very important factor that may influence the sensitivity of the immunoassay. In this case, according to the standard bioconjugation procedures, different amounts of mAb2 (0.2 μg~50 μg) was firstly loaded on the AuNPs (1 mL of the as-prepared colloidal AuNPs), and then 1 nmol of excess ODN was added to prepare the mAb2-AuNPs-ODN. As indicated from Fig. S3, the fluorescence signals of the MBs produced by the

same concentration of PSA (500 pg/mL) keep almost stable with the increase of mAb2 dosage from 0.2 μg/mL to 10 μg/mL, and then show a gradually decreasing tendency from 10 μg/mL to 50 μg/mL. This is probably because if too much mAb2 are firstly immobilized on the AuNPs, the capacity of the AuNPs for loading ODN will be inevitably decreased, which will obviously lower the efficiency of the TdT-catalyzed signal amplification. It should be noted that the signals of the blank without PSA almost keep constant irrespective of the variation of mAb2 amount. In consideration of both low detection limit of target PSA and high stability of the immunoreaction, 10 μg/mL mAb2 is selected for the preparation of mAb2-AuNPs-ODN conjugates in this work.

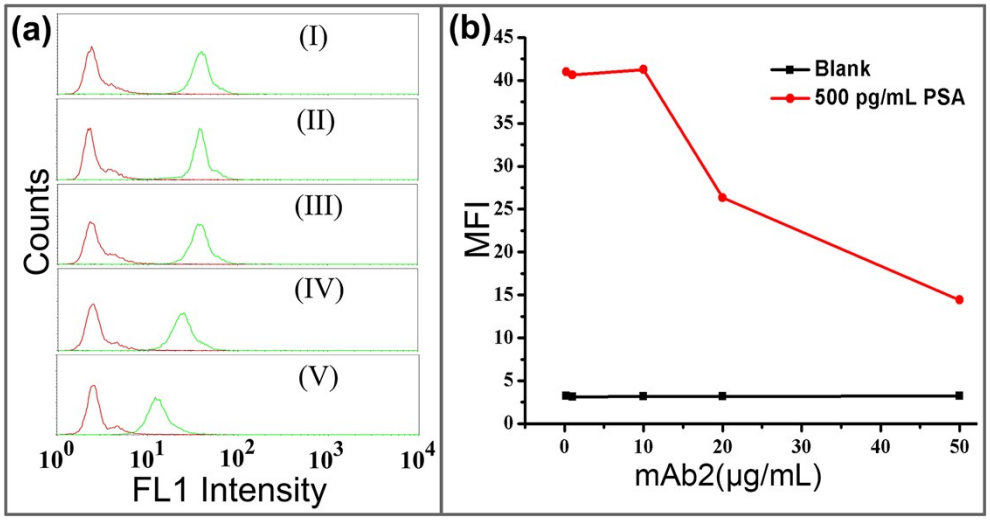

Fig. S3. Optimization of the ratio of mAb2/ODN on the AuNPs for the detection of PSA. (a) Fluorescence histograms of the MBs incubated with 500 pg/mL PSA (green) in comparison with those of blank control (red) in the presence of different mAb2 dosages (the amount of ODN is fixed at 1 nmol in the preparation of mAb2-AuNPs-ODN). The concentrations of mAb2: (I) 0.2 μg/mL; (II) 1 μg/mL; (III) 10 μg/mL; (IV) 20 μg/mL; (V) 50 μg/mL. (b) The corresponding S/B ratios with different mAb2 concentrations. S/B ratio refers to the ratio of the 500 pg/mL PSA-produced MFI value to that of blank control. The other experimental conditions: dTTP, 1 mM; TdT, 1 U; FL1 Voltage in the FCM measurement, 420 V.

4. Generality evaluation of the TdT-FCI for the detection of different antigens

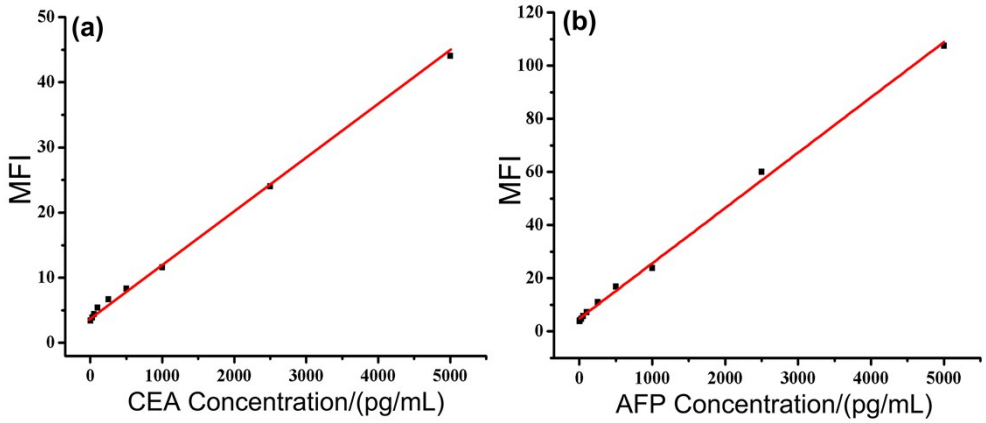

Fig. S4. (a) The relationship between the MFI values and CEA concentrations. (b) The relationship between the MFI values and AFP concentrations.

For the detection of CEA, the anti-CEA mAb1-conjugated MBs, and anti-CEA mAb2/ODN co-functionalized AuNPs were employed and the assay was conducted following the same procedures as those for PSA analysis using M-270 MBs as the reaction carrier. As shown in Fig. S4a, the MFI values are linearly proportional to the concentration of CEA in the range from 5 pg/mL to 5 ng/mL. The corresponding calibration equation is MFI=0.008C_{CEA}(pg/mL)+4.038 with a regression coefficient R of 0.9988. Following the same way, Fig. S4b exhibits the plot between the MFI values and AFP concentrations. The MFI values of the fluorescent MBs are linearly proportional to the concentration of AFP in the range from 5 pg/mL to 5 ng/mL. The correlation equation is MFI=0.021C_{AFP}(pg/mL)+4.782 with a correlation coefficient (R) of 0.9976. Therefore, one can see that by simply altering the target-specific antibodies, the proposed TdT-FCI possesses good generality to detect different protein targets. It is worth noting that the detection limits of PSA and CEA seem relatively higher than that of PSA, which should be possibly ascribed to the much larger molecular weight of AFP and CEA than PSA, as well as the affinity differences for the target-mediated immunoreactions.

5. Comparison of different analytical methods for PSA detection

Table S1. Comparison between the proposed TdT-FCI with other analytical methods for the detection of PSA.

Detection Strategy	Signal Readout	Detection Limit of PSA	References
AuNPs-based proximity immunoassay coupled with RNase H-based signal amplification	Fluorescence	1.25 pg/mL	S2
Bead-based immunoassay coupled with capillary-driven microfluidic chips	Fluorescence	3.6 pg/mL	S3
QD-based immunosensing/FRET	Luminescence	80 pg/mL	S4
Persistent luminescence nanoparticles-based FRET assay	Luminescence	90 pg/mL	S5
MBs-based enzyme-mediated reverse colorimetric immunoassay	Colorimetry	30 pg/mL	S6
1,4-Benzenediboronic-acid-induced AuNPs aggregation	Colorimetry	4 ng/mL	S7
Glucose oxidase-catalyzed growth of AuNPs	Colorimetry	~3.1 fg/mL	S8
Lanthanide-doped nanoprobes/Time resolved photoluminescence	Fluorescence	0.52 pg/mL	S9
Commercial dissociation-enhanced lanthanide fluoroimmunoassay (DELFIA) kit	Fluorescence	0.1 ng/mL	S10
MBs-supported immuno-PCR	Fluorescence	~3 pg/mL	S11
PSA aptamer coupled with guanine-based chemiluminescent biosensing	Chemiluminescence	1 ng/mL	S12
SERS nanotags	SERS	12-150 pg/mL	S13
SERS nanoprobes/Area-scanning method	SERS	0.11 pg/mL	S14
Phospholipid bilayer coated AuNPs label	MS	30 pg/mL	S15
Isotope tagging strategy	ICP-MS	240 pg/mL	S16
CQDs/g-C_3N_4 nanoheterostructures-based sensing platform coupled with	Photoelectrochemical (PEC)	5 pg/mL	S17

copper nanoclusters-assembled PSA aptamer			
RCA-synthesized nanoenzyme for the signal amplification	PEC	0.32 pg/mL	S18
Au nanocrystal decorated specific crystal facets $BiVO_4$ photoanode	PEC	4 pg/mL	S19
Enzymatic oxydate-triggered self-illuminated sensing platform	PEC	3 pg/mL	S20
Aptasensor based on a hairbrush-like gold nanostructure	Electrochemical	50 pg/mL	S21
Aptasensor based on GQDs-AuNRs modified screen-printed electrodes	Electrochemical	140 pg/mL	S22
DNA hybridization chain reaction (HCR) for signal amplification.	Electrochemical	0.17 pg/mL	S23
Coupling dielectrophoretic biomarker enrichment in nano-slit channel	Electrochemical	1-5 pg/mL	S24
Gold nanorods (AuNRs) and magnetic nanoparticles-based digital immunoassay	AuNRs Counting by dark field microscope	8 fg/mL	S25
A ‘‘signal-on’’ biosensor with positively charged gold nanoparticles as signal enhancer	Electrochemical	0.06 pg/mL	S26
A CeO_2-matrical enhancing sensing platform based on the Bi_2S_3-labeled inverted quenching mechanism	Electrochemiluminescence (ECL)	0.3 pg/mL	S27
Fluorescent immunosensor based on CuS nanoparticles	Fluorescence	0.1 pg/mL	S28
TdT-FCI	Fluorescence/flow cytometry	0.5 pg/mL	This work

References

S1 G. Frens, *Nat. Phys. Sci.*, 1973, **241**, 20-22.

S2 J. Xu, M. Shi, W. Chen, Y. Huang, L. Fang, L. Yao, S. Zhao, Z.-F. Chen and H. Liang, *Chem.*

Commun., 2018, **54**, 2719-2722.

S3 Y. Temiz, M. Lim and E. Delamarche, *Proc. SPIE.*, 2016, **9705**, 97050Z.

S4 S. Bhuckory, L. Mattera, K. D. Wegner, X. Qiu, Y.-T. Wu, L. J. Charbonnière, P. Reiss and N. Hildebrandt, *Chem. Commun.*, 2016, **52**, 14423-14425.

S5 B.-Y. Wu and X.-P. Yan, *Chem. Commun.*, 2015, **51**, 3903-3906.

S6 Z. Gao, M. Xu, L. Hou, G. Chen and D. Tang, *Anal. Chem.*, 2013, **85**, 6945-6952.

S7 Y.-C. Yang and W.-L. Tseng, *Anal. Chem.*, 2016, **88**, 5355-5362.

S8 D. Liu, J. Yang, H.-F. Wang, Z. Wang, X. Huang, Z. Wang, G. Niu, A. R. Hight Walker and X. Chen, *Anal. Chem.*, 2014, **86**, 5800-5806.

S9 J. Xu, S. Zhou, D. Tu, W. Zheng, P. Huang, R. Li, Z. Chen, M. Huang and X. Chen, *Chem. Sci.*, 2016, **7**, 2572-2578.

S10 K. Järås, B. Adler, A. Tojo, J. Malm, G. Marko-Varga, H. Lilja and T. Laurell, *Clin. Chim*. *Acta*, 2012, **414**, 76-84.

S11 X. Jiang, S. Cheng, W. Chen, L. Wang, F. Shi and C. Zhu, *Anal. Biochem.*, 2012, **424**, 1-7.

S12 T. Cha, S. Cho, Y. T. Kim and J. H. Lee, *Biosens. Bioelectron.*, 2014, **61**, 31-37.

S13 Z. Cheng, N. Choi, R. Wang, S. Lee, K. C. Moon, S.-Y. Yoon, L. Chen and J. Choo, *ACS Nano,* 2017, **11**, 4926-4933.

S14 H. Chang, H. Kang, E. Ko, B.-H. Jun, H. Y. Lee, Y.-S. Lee and D. H. Jeong, *ACS Sens.*, 2016, **1**, 645-649.

S15 X.-C. Lin, X.-N. Wang, L. Liu, Q. Wen, R.-Q. Yu and J.-H. Jiang, *Anal. Chem.*, 2016, **88**, 9881-9884.

S16 G. Sun, B. Huang, Y. Zhang, Y. Zhang, Z. Xing, S. Zhang and X. Zhang, *Chem. Commun.*, 2017, **53**, 13075-13078.

S17 S. Lv, Y. Li, K. Zhang, Z. Lin and D. Tang, *ACS Appl. Mater. Interfaces*, 2017, **9**, 38336-38343.

S18 J. Zhuang, D. Tang, W. Lai, M. Xu and D. Tang, *Anal. Chem.*, 2015, **87**, 9473-9480.

S19 J. Shu, Z. Qiu, Z. Lin, G. Cai, H. Yang and D. Tang, *Anal. Chem.*, 2016, **88**, 12539-12546.

S20 J. Shu, Z. Qiu, Q. Zhou, Y. Lin, M. Lu and D. Tang, *Anal. Chem.*, 2016, **88**, 2958-2966.

S21 N. Sattarahmady, A. Rahi and H. Heli, *Sci. Rep.*, 2017, **7**, 11238.

S22 M. Srivastava, N. R. Nirala1, S. K. Srivastava and R. Prakash, *Sci. Rep.*, 2018, **8**, 1923.

S23 J. Guo, J. Wang, J. Zhao, Z. Guo and Y. Zhang, *ACS Appl. Mater. Interfaces*, 2016, **8**, 6898-6904.

S24 B. J. Sanghavi, W. Varhue, A. Rohani, K.-T. Liao, L. A. L. Bazydlo, C.-F. Chou and N. S. Swami, *Lab Chip*, 2015, **15**, 4563-4570.

S25 L. Zhu, G. Li, S. Sun, H. Tan and Y. He, *RSC Adv.*, 2017, **7**, 27595-27602.

S26 D. Wang, Y. Zheng, Y. Chai, Y. Yuan and R. Yuan, *Chem. Commun.*, 2015, **51**, 10521-10523.

S27 Y. Zhao, Q. Wang, J. Li, H. Ma, Y. Zhang, D. Wu, B. Du and Q. Wei, *J. Mater. Chem. B*, 2016, **4**, 2963-2971.

S28 Y.-D. Zhu, J. Peng, L.-P. Jiang and J.-J. Zhu, *Analyst*, 2014, **139**, 649-655.